Available online at www.sciencedirect.com
ScienceDirect
ELSEVIER
Earth and Planetary Science Letters xx (2006) xxx–xxx
EPSL
www.elsevier.com/locate/epsl

The role of radiogenic heat production in the thermal evolution of a Proterozoic granulite-facies orogenic belt: Eastern Ghats, Indian Shield

P. Senthil Kumar *, Rajeev Menon, G.K. Reddy

National Geophysical Research Institute, Uppal Road, Hyderabad 500 007, India

Received 7 February 2006; received in revised form 25 October 2006; accepted 10 November 2006

Editor: C.P. Jaupart

Abstract

The Eastern Ghats Belt (EGB) is a deeply eroded Proterozoic orogenic belt juxtaposed against the Archaean Dharwar–Bastar–Singhbhum cratons in the Indian Shield. The tectono-metamorphic history of this belt is broadly similar to the Grenvillian orogenic belts. The EGB exposes dominantly the granulite-facies rocks such as charnockites, khondalites and migmatitic gneisses with less abundant intermediate to mafic granulites. The granulites are intruded by small plutons of granites, syenites and anorthosites. The northern and southern parts of the belt (NEGB and SEGB) have distinct crustal histories, but 1600–1000–550 Ma old tectono-metamorphic events are common to both the belts. In this research, we attempt to understand the present-day and past thermal state of this orogen on the basis of our radioelement (K, U and Th) measurements at 562 sites using in-situ gamma-ray spectrometry, with other geological and geophysical constraints. The dominant rock types of the NEGB and SEGB have similar radioelement abundances (>3% K, 3 ppm U and 30 ppm Th) and heat production. Heat production of charnockites, gneisses, khondalites and intermediate granulites of the NEGB is 2.9, 2.8, 2.9 and 1.1 $\mu W\ m^{-3}$, respectively. In the SEGB, they are 2.7, 2.5, 2.8 and 0.6 $\mu W\ m^{-3}$, respectively, and the mafic granulites are the lowest in heat production (0.3 $\mu W\ m^{-3}$). On the basis of the heat production data and crustal petrologic models, we show that the crustal contribution of the NEGB and SEGB is 54 and 45 $mW\ m^{-2}$, respectively, which are broadly in good agreement with the available surface heat flow data. Thermal models of the present-day EGB crust indicate that the temperature at the Moho is ~550 °C. Radioelements and heat production of the Eastern Ghats granulites are higher than the other granulite belts in the Indian shield. The crustal radiogenic heat contribution and Moho temperatures of the EGB are higher than the adjoining Archaean cratons. This could also be responsible for the development of inverted metamorphic isograds in the tectonic boundary between the EGB and the adjoining cratons during a collisional orogenic event at about 550 Ma ago.

Keywords: radioelements; heat production; thermal evolution; Proterozoic granulites; Eastern Ghats Belt; Indian Shield

1. Introduction

In continental lithosphere, the thermal structure is mainly controlled by the nature of depth distribution of heat producing elements (K, U and Th), which are largely concentrated in the crust, and contribute significantly to the overall heat flow (e.g. [1]). Several studies have been attempted to understand the nature of radiogenic heat production distribution within the crust, particularly, along the exposed crustal cross-sections that provided an excellent opportunity to sample the various rock types

* Corresponding author. Tel.: +91 40 23434632; fax: +91 40 27171564.
E-mail address: senthilngri@yahoo.com (P.S. Kumar).

0012-821X/$ - see front matter © 2006 Elsevier B.V. All rights reserved.
doi:10.1016/j.epsl.2006.11.018

constituting the crust [2–7]. Among the crustal lithologies, the granulite-facies rocks represent the middle- to lower-continental crust, and therefore provide an insight to the composition and evolution of the deeper parts of the crust [8,9]. Although upper crustal rocks have been sampled well everywhere (see [10]), the deeper crustal rocks can be studied only from the crustal cross-sections exposing the granulite-facies rocks, and those found as xenoliths in basalts and kimberlites [11]. As xenolithic samples may not be representative of the entire lower crust, the exposed sections provide better constraints on the deeper crustal composition. In addition, the granulite-facies rocks shed light on the thermal evolution of the deeper crust and provide an opportunity to characterize its thermal properties, for example, heat production distribution [2–4,6].

Geochemical and petrological studies show that, as a result of high-grade metamorphism, large-ion lithophile elements including the heat producing elements (K, U and Th) are often removed significantly from the granulites (see [12]), either due to partial melting (e.g. [13]) or fluid–rock interaction (e.g. [14]). Heat flow and heat production studies over the various granulite provinces indicate that the granulites are low heat producing (average of ~0.4 μW m^{-3}); as a result, the granulitic crust contributes less to heat flow (e.g. [15,16]). It appears that these inferences are suitable to some of the Archaean provinces only. On the other hand, Proterozoic orogens exposing granulites have not been studied thoroughly in terms of heat production distribution. As these orogens evolved in a different manner compared to the adjoining Archaean cratons, examining their thermal structure is important. Also, there is a great need to evaluate the role of radiogenic heat production in the thermal evolution of such orogens, as it plays a crucial role in driving crustal metamorphism [17–20].

The Eastern Ghats Belt (EGB) is a deeply eroded part of a Proterozoic orogen exposing one of the largest granulite-facies terrains in the Indian Shield (Fig. 1). Extensive geochemical, petrological and geochronological studies have been carried out in this belt (see [21]), which have improved our understanding of the Proterozoic crustal evolution, but there is no detailed study on the radioelement and heat production distribution in this belt. Therefore, in this study, we present radioelement (K, U and Th), and heat production characteristics of the granulite-facies rocks exposed in the Eastern Ghats Belt. Based on these data and other geological and geophysical constraints, we model the crustal thermal structure of the present-day EGB and for the past (~550 Ma ago) to understand the thermal history of this orogen.

2. Geology

The Eastern Ghats Belt is ~900 km long and >300 km wide in the northern part and a few tens of kilometers wide in the southern part (Fig. 2). Dobmeier and Raith [21] have summarized the geological history of the belt. Major rock types are khondalites (quartz–K feldspar–biotite–garnet–sillimanite±graphite), charnockites (quartz–K feldspar–orthopyroxene–clinopyroxene–garnet±biotite± amphibole), migmatitic gneisses (quartz–K feldspar–biotite–amphibole) with less dominant intermediate

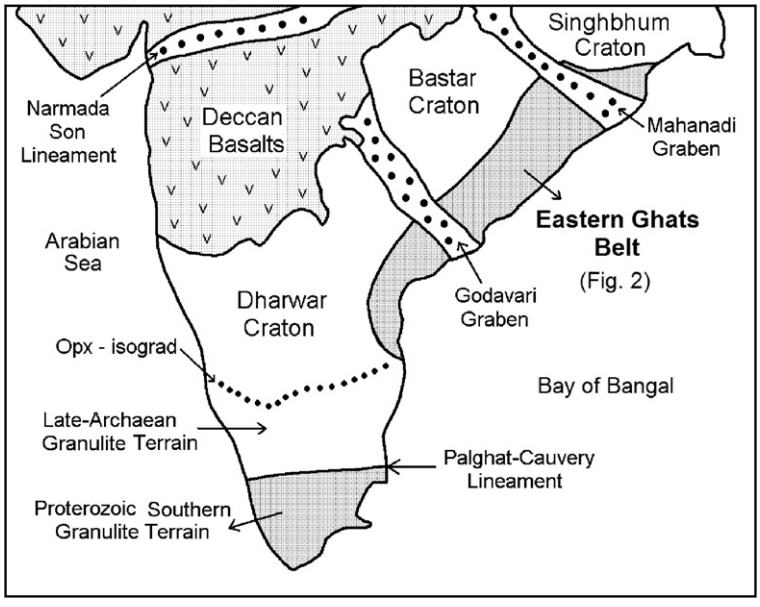

Fig. 1. Sketch map of the Indian Shield showing the location of the Eastern Ghats Belt.

Please cite this article as: P.S. Kumar et al., The role of radiogenic heat production in the thermal evolution of a Proterozoic granulite-facies orogenic belt: Eastern Ghats, Indian Shield, Earth Planet. Sci. Lett. (2006), doi:10.1016/j.epsl.2006.11.018

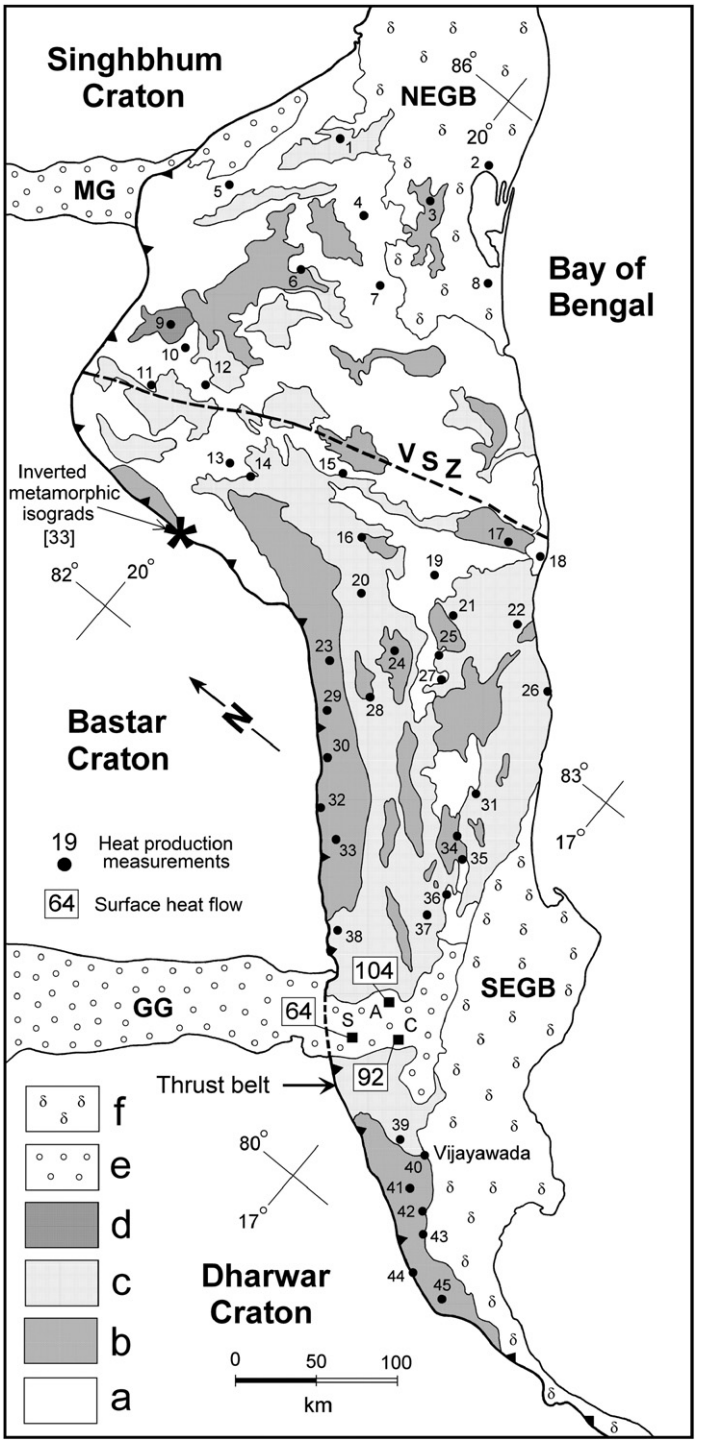

Fig. 2. Geological map of the Eastern Ghats Belt [38]. Rock types: a — gneisses, b — charnockites, c — khondalites, d — anorthosites, e — Gondwana sedimentary rocks, and f — alluvium. The Eastern Ghats Belt is juxtaposed against the Dharwar–Bastar–Singhbhum cratons along a thrust zone. The belt is dissected by Godavari (GG) and Mahanadi (MG) grabens. Heat flow values (mW m^{-2}) are shown in the open rectangles (S — Sattupalli, A — Aswaraopet, and C — Chintalapudi). NEGB — Northern Eastern Ghats Belt, SEGB — Southern Eastern Ghats Belt, and VSZ — Vamsadara Shear Zone. The localities, in the vicinity of which a number of in-situ analyses could be grouped together, have been shown as a number in the map. Locality names and radioelement and heat production data are given in Table 1.

Please cite this article as: P.S. Kumar et al., The role of radiogenic heat production in the thermal evolution of a Proterozoic granulite-facies orogenic belt: Eastern Ghats, Indian Shield, Earth Planet. Sci. Lett. (2006), doi:10.1016/j.epsl.2006.11.018

Table 1
Radioelement and heat production characteristics of various rock types in the Eastern Ghats Belt

Map no.	Stations	*N*	Mean Th (ppm)	Mean U (ppm)	Mean K (%)	Th/U	Mean HP, present-day	Mean HP, 550 Ma ago
The Northern Eastern Ghats Belt (NEGB)								
Charnockites:								
1	Angul	4	6.39 (1.68)	2.45 (0.12)	2.51 (0.49)	2.61	1.46 (0.15)	1.63 (0.16)
2	Tangi	3	19.88 (4.32)	2.23 (0.74)	4.63 (1.16)	8.91	2.36 (0.57)	2.61 (0.64)
3	Nayagarh	12	27.56 (5.49)	1.38 (0.13)	3.81 (0.26)	19.97	2.59 (0.41)	2.81 (0.43)
4	Dasphalla	11	28.03 (5.22)	2.24 (0.29)	4.36 (0.36)	12.51	2.89 (0.43)	3.15 (0.45)
6	Phulbani	19	28.12 (3.33)	2.65 (0.18)	4.61 (0.19)	10.61	3.02 (0.26)	3.31 (0.27)
7	Bhanjanagar	14	31.11 (3.96)	2.57 (0.35)	4.81 (0.16)	12.11	3.23 (0.33)	3.52 (0.34)
8	Boira	6	38.90 (5.13)	2.17 (0.21)	3.86 (0.38)	17.93	3.57 (0.35)	3.83 (0.37)
	All data	69	28.07 (3.38)	2.28 (0.27)	4.28 (0.52)	12.31	2.90 (0.35)	3.16 (0.38)
Gneisses:								
1	Angul	7	23.43 (6.60)	1.62 (0.22)	3.73 (0.50)	14.48	2.36 (0.48)	2.58 (0.50)
2	Tangi	4	31.62 (2.47)	3.21 (0.91)	3.15 (0.68)	9.85	3.27 (0.43)	3.53 (0.48)
5	Boinda	14	25.37 (3.13)	1.85 (0.24)	3.64 (0.34)	13.71	2.54 (0.28)	2.76 (0.30)
10	Deogan	5	28.98 (7.46)	3.63 (1.44)	4.50 (0.24)	7.98	3.32 (0.30)	3.63 (0.31)
11	Patnagarh	8	32.60 (5.42)	2.06 (0.12)	3.44 (0.20)	15.83	3.07 (0.38)	3.31 (0.39)
12	Saintala	8	25.79 (4.24)	1.92 (0.29)	4.87 (0.29)	13.43	2.70 (0.36)	2.97 (0.37)
	All data	46	27.34 (1.96)	2.18 (0.21)	3.88 (0.17)	12.57	2.78 (0.15)	3.03 (0.16)
Khondalites:								
1	Angul	2	18.72	1.63	3.03	11.52	1.98	2.16
8	Boira	2	29.68	2.02	2.33	14.69	2.50	2.63
10	Deogan	3	32.65 (2.97)	2.59 (0.68)	3.70 (0.17)	12.61	3.23 (0.25)	3.49 (0.26)
11	Patnagarh	3	36.06 (3.79)	2.05 (0.12)	2.74 (0.23)	17.59	3.24 (0.24)	3.46 (0.24)
12	Saintala	8	28.35 (4.03)	2.27 (0.26)	3.68 (0.39)	12.49	2.86 (0.28)	3.10 (0.28)
	All data	18	29.43 (2.19)	2.18 (0.16)	3.31 (0.24)	13.50	2.87 (0.16)	3.10 (0.16)
Intermediate granulites:								
3	Nayagarh	2	15.73	0.94	1.04	16.82	1.43	1.52
12	Saintala	3	7.60 (1.98)	0.58 (0.14)	0.65 (0.28)	13.10	0.73 (0.16)	0.79 (0.17)
	All data	5	10.85 (2.90)	0.72 (0.18)	0.81 (0.21)	15.07	1.01 (0.21)	1.08 (0.21)
Anorthosites:								
9	Balangir	15	2.04 (0.30)	0.52 (0.08)	0.67 (0.02)	3.92	0.36 (0.04)	0.41 (0.04)
The Southern Eastern Ghats Belt (SEGB)								
Charnockites:								
14	Bhawanipatna	16	36.37 (3.06)	1.56 (0.13)	3.85 (0.21)	23.31	3.24 (0.22)	3.48 (0.23)
15	Muniguda	4	33.17 (3.14)	5.59 (1.32)	2.63 (0.38)	5.93	3.93 (0.41)	4.25 (0.44)
16	Rayagada	11	33.80 (3.60)	1.62 (0.19)	3.68 (0.27)	20.86	3.06 (0.25)	3.30 (0.26)
17	Palakonda	7	37.75 (6.75)	2.17 (0.57)	3.62 (0.23)	17.40	3.47 (0.48)	3.79 (0.50)
18	Srikakulam	6	25.93 (6.53)	1.21 (0.17)	3.15 (0.21)	21.43	2.37 (0.48)	2.56 (0.50)
19	Parvathipuram	8	18.43 (3.90)	1.59 (0.09)	3.70 (0.16)	11.59	2.00 (0.27)	2.21 (0.28)
20	Lakshmipur	16	34.22 (5.87)	1.57 (0.14)	3.67 (0.12)	21.80	3.08 (0.41)	3.31 (0.42)
21	Bobbilli	5	24.95 (7.52)	1.90 (0.50)	4.16 (0.19)	13.13	2.58 (0.58)	2.82 (0.60)
22	Vizianagaram	9	33.38 (6.96)	2.84 (0.40)	4.23 (0.27)	11.75	3.40 (0.58)	3.68 (0.61)
23	Koraput	6	18.77 (5.12)	1.09 (0.17)	3.62 (0.35)	17.22	1.90 (0.39)	2.08 (0.40)
24	Sunabeda	13	13.57 (3.08)	2.21 (0.17)	4.44 (0.35)	6.14	2.45 (0.22)	2.62 (0.23)
25	Anantagiri	15	19.64 (3.49)	1.44 (0.23)	3.50 (0.26)	13.64	2.03 (0.29)	2.23 (0.31)
28	Lamtaput	7	29.69 (15.3)	1.77 (0.48)	4.06 (0.44)	16.77	2.86 (1.19)	3.10 (1.24)
29	Boipariguda	5	17.24 (4.06)	2.09 (0.36)	2.72 (0.21)	8.25	1.96 (0.34)	2.15 (0.35)
30	Mattili	7	29.93 (6.72)	2.58 (0.65)	3.89 (0.17)	11.60	3.06 (0.55)	3.33 (0.58)
31	K. D. Pet	6	31.36 (8.05)	1.13 (0.37)	3.75 (0.42)	27.75	2.78 (0.62)	3.00 (0.64)
32	Malkangiri	10	24.28 (10.6)	2.65 (0.79)	4.14 (0.33)	9.16	2.72 (0.84)	2.98 (0.88)
33	Kalimela	14	40.06 (6.71)	2.51 (0.62)	3.72 (0.25)	15.96	3.72 (0.58)	3.99 (0.61)
34	Koyyuru	9	30.21 (4.55)	0.99 (0.14)	2.87 (0.26)	30.52	2.58 (0.35)	2.76 (0.37)
35	Jadangi	7	31.61 (10.4)	0.95 (0.22)	3.27 (0.20)	33.27	2.71 (0.76)	2.90 (0.78)
36	Addateegala	4	31.66 (6.84)	0.87 (0.31)	2.87 (0.81)	36.39	2.65 (0.51)	2.83 (0.54)
37	R. C. Varam	8	43.66 (9.68)	1.14 (0.22)	3.95 (0.35)	38.30	3.64 (0.70)	3.89 (0.73)
38	Chinturu	9	23.49 (4.02)	2.98 (0.64)	3.88 (0.28)	7.88	2.72 (0.28)	2.99 (0.30)

Please cite this article as: P.S. Kumar et al., The role of radiogenic heat production in the thermal evolution of a Proterozoic granulite-facies orogenic belt: Eastern Ghats, Indian Shield, Earth Planet. Sci. Lett. (2006), doi:10.1016/j.epsl.2006.11.018

Table 1 (*continued*)

Map no.	Stations	*N*	Mean Th (ppm)	Mean U (ppm)	Mean K (%)	Th/U	Mean HP, present-day	Mean HP, 550 Ma ago
The Southern Eastern Ghats Belt (SEGB)								
Charnockites:								
39	Kondapalli	13	26.94 (5.55)	2.20 (0.41)	3.86 (0.30)	12.25	2.76 (0.43)	3.00 (0.45)
41	Amaravathi	3	32.11 (19.4)	0.69 (0.10)	2.53 (0.31)	46.54	2.61 (1.29)	2.77 (1.31)
42	Perecherla	12	29.06 (6.01)	1.91 (0.23)	3.31 (0.24)	15.21	2.78 (0.43)	3.00 (0.44)
43	Kondaveedu	18	22.62 (4.62)	1.71 (0.20)	4.03 (0.30)	13.23	2.36 (0.33)	2.58 (0.34)
44	Kotappakonda	13	30.33 (7.84)	1.73 (0.20)	3.57 (0.33)	17.53	2.84 (0.56)	3.07 (0.58)
45	Ramkuru	10	19.51 (5.25)	1.00 (0.13)	2.85 (0.28)	19.51	1.85 (0.34)	2.01 (0.34)
	All data	271	28.33 (1.26)	1.80 (0.08)	3.63 (0.06)	15.74	2.73 (0.10)	2.96 (0.10)
Gneisses:								
17	Palakonda	4	28.84 (1.98)	2.12 (0.29)	3.51 (0.09)	13.60	2.84 (0.08)	3.07 (0.07)
18	Srikakulam	4	17.56 (5.12)	1.30 (0.19)	3.25 (0.05)	13.51	1.83 (0.39)	2.01 (0.40)
22	Vizianagaram	5	27.18 (4.93)	2.61 (0.47)	2.00 (0.68)	10.41	2.71 (0.42)	2.90 (0.44)
25	Anantagiri	4	28.95 (7.00)	1.06 (0.07)	2.40 (0.22)	27.31	2.47 (0.49)	2.64 (0.51)
	All data	17	25.75 (2.57)	1.82 (0.22)	2.74 (0.25)	14.13	2.47 (0.20)	2.67 (0.21)
Khondalites:								
26	Visakhapatnam	21	31.39 (1.79)	1.79 (0.15)	1.88 (0.35)	17.54	2.78 (0.17)	2.95 (0.19)
31	K. D. Pet	3	36.64 (3.10)	2.57 (0.24)	2.17 (0.25)	14.26	3.36 (0.23)	3.58 (0.24)
34	Koyyuru	4	26.62 (2.78)	1.09 (0.34)	2.96 (0.20)	24.42	2.37 (0.22)	2.55 (0.23)
36	Addateegala	12	26.57 (3.42)	1.91 (0.18)	2.99 (0.21)	13.91	2.58 (0.27)	2.78 (0.28)
37	R. C. Varam	7	30.33 (3.92)	1.65 (0.13)	1.91 (0.49)	18.38	2.67 (0.26)	2.84 (0.27)
40	Vijayawada	9	32.15 (1.29)	2.26 (0.26)	2.85 (0.16)	14.23	3.04 (0.13)	3.26 (0.14)
	All data	56	30.29 (1.17)	1.87 (0.09)	2.37 (0.17)	16.20	2.76 (0.10)	2.96 (0.11)
Intermediate granulites:								
20	Lakshmipur	2	4.61	0.72	1.04	6.44	0.60	0.67
23	Koraput	8	3.26 (0.38)	0.68 (0.08)	0.90 (0.13)	4.79	0.49 (0.05)	0.54 (0.05)
24	Sunabeda	4	5.63 (0.34)	1.20 (0.25)	1.09 (0.10)	4.69	0.80 (0.08)	0.89 (0.09)
27	Araku	7	3.23 (0.40)	0.66 (0.13)	1.14 (0.20)	4.89	0.50 (0.07)	0.56 (0.08)
28	Lamtaput	4	0.96 (0.27)	0.66 (0.14)	0.59 (0.19)	1.45	0.29 (0.04)	0.33 (0.05)
32	Malkangiri	3	5.58 (2.26)	0.67 (0.12)	1.02 (0.15)	8.33	0.66 (0.20)	0.72 (0.21)
39	Kondapalli	6	5.52 (0.76)	0.41 (0.04)	1.55 (0.09)	13.46	0.63 (0.07)	0.71 (0.07)
41	Amaravathi	5	4.56 (1.25)	0.67 (0.07)	1.56 (0.20)	6.81	0.63 (0.10)	0.71 (0.11)
42	Perecherla	2	0.27	0.21	1.17	1.29	0.18	0.23
44	Kotappakonda	2	6.39	0.54	0.52	11.82	0.63	0.68
	All data	43	4.02 (0.36)	0.66 (0.05)	1.12 (0.07)	6.00	0.55 (0.03)	0.62 (0.04)
Mafic granulites:								
13	Karlapada	8	1.66 (0.68)	1.19 (0.90)	1.13 (0.91)	1.39	1.11 (0.92)	1.13 (0.91)
45	Ramkuru	5	2.12 (0.95)	0.32 (0.14)	0.30 (0.14)	6.63	0.28 (0.12)	0.30 (0.13)
	All data	13	1.83 (0.49)	0.33 (0.04)	0.28 (0.07)	5.55	0.26 (0.05)	0.28 (0.05)
Leptynites:								
	All data	9	25.02 (3.78)	5.00 (3.46)	4.38 (0.20)	5.00	3.43 (0.82)	3.73 (0.91)

Standard error of the mean is given in parenthesis. *N* is number of measurements. Unit of heat production (HP) is $\mu W\ m^{-3}$.

granulites (quartz–plagioclase–clinopyroxene–orthopyroxene–garnet) and mafic granulites (plagioclase–clinopyroxene–orthopyroxene–garnet). Small plutons of granites, alkaline rocks, and anorthosites intrude these granulites, mostly along the western margin of the EGB.

Based on the isotopic geochemical studies of Rickers et al. [22], we divide the Eastern Ghats into the northern Eastern Ghats Belt (NEGB) and southern Eastern Ghats Belt (SEGB) with the Vamsadara Shear Zone (VSZ) being their notional boundary (Fig. 2). The NEGB includes the area between the VSZ and the Mahanadi graben, where Nd model ages of the granulites are largely Proterozoic (~2200–1800 Ma old). In contrast, the granulites of the SEGB, which are exposed to the north (up to the VSZ) and south of the Godavari graben, have Archaean (~3900–2500 Ma old) Nd model ages. However, both these belts have undergone polyphase deformation [23,24], and three episodes of regional metamorphic events: 1600 Ma and 1000 Ma old granulite-facies metamorphism, and ~550 Ma old amphibolite-facies metamorphism [22,25–28], whose imprints are not preserved uniformly in all places. The granulites of the NEGB and SEGB record peak metamorphic pressures from ~8 to 12 kbars, and peak

Please cite this article as: P.S. Kumar et al., The role of radiogenic heat production in the thermal evolution of a Proterozoic granulite-facies orogenic belt: Eastern Ghats, Indian Shield, Earth Planet. Sci. Lett. (2006), doi:10.1016/j.epsl.2006.11.018

temperatures from ~800 °C up to >1000 °C, showing variable retrograde *P–T* paths (clockwise and anticlockwise paths) [29]. Notably this belt has undergone ultrahigh temperature (UHT) metamorphism reaching >1000 °C, at several places. Although the ages of these metamorphic events are not fully established, the available isotope geochronologic data clearly suggest that the western margins of the NEGB and SEGB are dominated by the imprints of 1600 Ma old granulite-facies metamorphism, and the eastern parts record ~1000 Ma old granulite-facies and ~550 Ma old amphibolite-facies metamorphic events (e.g. [26]).

The EGB is cut by NW–SE trending linear rift zones, the Mahanadi and Godavari grabens in the north and south, respectively, which are the locales of Paleozoic–Mesozoic Gondwana sedimentation, and are associated with extensive coal deposits and hydrocarbon occurrences (e.g. [30]). The EGB is juxtaposed against the middle to late Archaean Dharwar–Bastar–Singhbhum cratons. The time of amalgamation event has not been clearly constrained. However, in the absence of 1600 and 1000 Ma old metamorphic events in the vicinity of the adjoining cratons, it appears that the amalgamation could have been between 850 Ma and 550 Ma ago (e.g. [31,32]). A thrust fault, whose sense of displacement is top-to-west, marks the boundary between the EGB and the adjoining cratons. The footwall cratonic rocks close to the thrust belt preserve inverted metamorphic isograds, and the terrains on either side are characterized by distinct metamorphic *P–T* histories [33].

In recent years, in the framework of the Rodina Supercontinent reconstruction, the EGB was correlated with Enderby Land of the eastern Antarctica, on the basis of the metamorphic rocks characterized by similar *P–T–t* evolution (e.g. [29,34]), denudation and thermal histories (e.g. [26,28,35]), and isotopic geochemical systematics (e.g. [22]). Therefore, in most of the palaeo-geographic reconstructions of the Gondwana, from the time middle Proterozoic to Mesozoic, the EGB is considered to be an integral part of the eastern Antarctica that consists of the Rayner Complex, the Mawson Coast area, the Prydz Bay and the Northern Charles Mountains (see also [36]). Lithosphere along the eastern margin of the EGB is found to be thinner compared to the adjoining regions because of the effect of Indo-Antarctic rifting around 120 Ma ago [37].

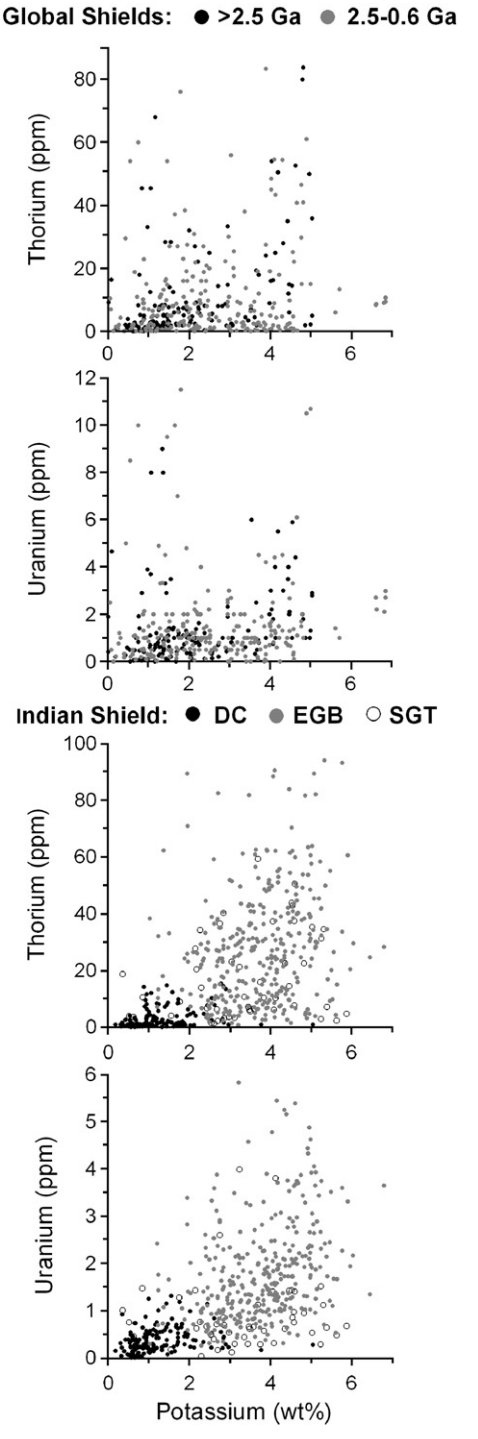

Fig. 3. K, U and Th distributions in the Archaean and Proterozoic granulites of the global shields (data from the sources of Fig. 5) and in the Indian Shield (data of this study, Kumar and Reddy [6] and Ray et al. [16]). DC — Dharwar Craton (Archaean), EGB — Eastern Ghats Belt (Proterozoic), and SGT — Southern Granulite Terrain (Proterozoic).

3. Data

3.1. Gamma-ray spectrometry

We have determined the concentration of radioelements (K, U and Th) in the field using a SCINTREX

Please cite this article as: P.S. Kumar et al., The role of radiogenic heat production in the thermal evolution of a Proterozoic granulite-facies orogenic belt: Eastern Ghats, Indian Shield, Earth Planet. Sci. Lett. (2006), doi:10.1016/j.epsl.2006.11.018

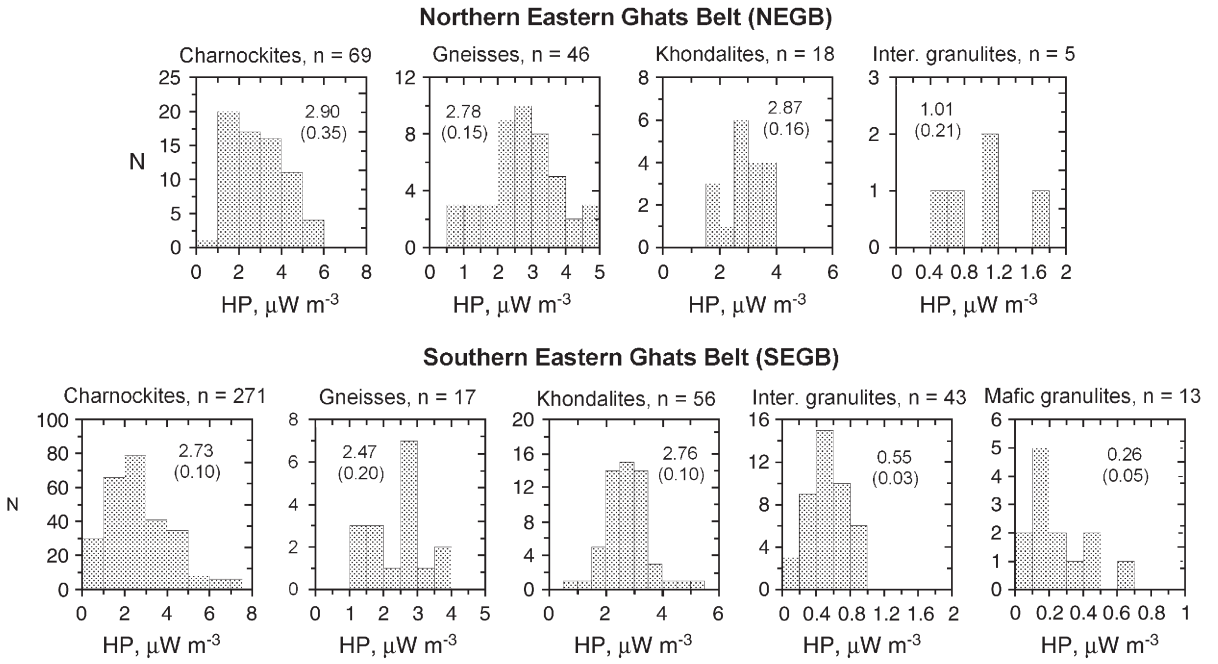

Fig. 4. Heat production data of the granulites of the Eastern Ghats Belt. Mean and standard error are shown in parenthesis.

gamma-ray spectrometer that contains a 113-cubic-inch NaI(Tl) crystal as sensor. Count rates were obtained from the four channels of a stabilized gamma-ray spectrum. The method is the same as described by Ray et al. [16] Count time was generally set for 300 s for the rock types enriched in radiolements (e.g., charnockites, khondalites, and gneisses), and was increased to 600 s in the case of rock types that are depleted in radioelement abundance (e.g., anorthosites and intermediate to mafic granulites). The errors in general do not exceed 2% for K and 5% for U and Th. The outcrops studied expose un-weathered rocks (fresh quarry surfaces), which satisfy 2π geometry requirements. It is worth mentioning here that the results of the in-situ gamma-ray spectrometry are in good agreement with the results obtained by XRF for K and INAA for U and Th, both at the low (0.5% K, 0.5 ppm Th and 0.2 ppm U) (see [16]) and high concentration levels (K > 3%, U > 2 ppm and Th > 10 ppm). Considering the in-situ gamma-ray spectrometry used in this study, it is possible that secular disequilibrium has some effect on the U measurements, and its impact may vary from place to place depending on the nature of fluid–rock interaction (see [5,39]). Ketcham [39] suggests a method for detection and correction for the secular disequilibrium. This method could not be applied due to the limitations in the in-situ gamma-ray spectrometry used here. Therefore, we indicate that the U determinations could be slightly underestimates. In this study, we have determined radioelement abundances at 562 sites, which include the rock formations such as charnockites (n = 340), gneisses (n = 63), khondalites (n = 74), intermediate granulites (n = 48), mafic granulites (n = 13), leptynites (n = 9) and anorthosites (n = 15), covering both the NEGB and SEGB (Table 1).

3.2. Radioelements

The radioelement data (K, U and Th) of the EGB are presented in Table 1. In the NEGB and SEGB, the dominant granulite-facies rocks–charnockites, gneisses and khondalites are enriched in radioelements (3% K, 3 ppm U and >30 ppm Th), while the intermediate to mafic granulites are depleted (Table 1). When the radioelement data of granulites of the NEGB and SEGB are compared, they have broadly similar radioelement abundances including the elemental ratios (Table 1), although the protolithic ages and isotopic geochemical evolution of these two belts are shown to be different [22]. In these rocks, K is mainly hosted in K-feldspar and biotite, while the accessory minerals such as monazite, zircon, and apatite are the main carriers of U and Th. Also, the EGB granulites form the main source of beach-placer deposits of radioactive minerals (e.g., monazite and zircon) along the east coast of India [40,41]. Another observation is that the EGB granulites are characterized by high Th/U ratios (Table 1). It may be related to the effect of polyphase high-grade metamorphic events in the EGB, as the granulite-facies metamorphism greatly

Please cite this article as: P.S. Kumar et al., The role of radiogenic heat production in the thermal evolution of a Proterozoic granulite-facies orogenic belt: Eastern Ghats, Indian Shield, Earth Planet. Sci. Lett. (2006), doi:10.1016/j.epsl.2006.11.018

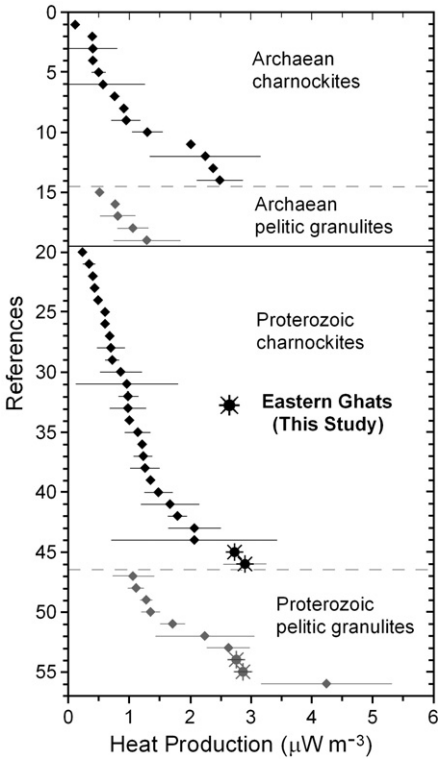

Fig. 5. Heat production of the Archaean and Proterozoic granulites world-wide. References: 1—[48], 2—[6], 3—[49], 4—[4], 5—[2], 6—[50], 7—[51], 8—[51], 9—[52], 10—[53], 11—[54], 12—[54], 13—[55], 14—[56,57], 15—[58], 16—[4], 17—[59], 18—[59], 19—[59], 20—[60], 21—[61], 22—[3], 23—[62], 24—[63], 25—[3], 26—[3], 27—[64], 28—[65], 29—[66], 30—[67], 31—[50], 32—[68], 33—[62], 34—[50], 35—[69], 36—[70], 37—[16], 38—[71], 39—[50], 40—[72], 41—[73], 42—[61], 43—[66], 44—[53], 45—SEGB [this study], 46—NEGB [this study], 47—[74], 48—[16], 49—[75], 50—[42,76], 51—[72], 52—[50], 53—[16], 54—SEGB [this study], 55—NEGB [this study], and 56—[77]. Andreoli et al. [78] report very high heat producing granulites from the Proterozoic Namaqualand belt, South Africa, which is not shown in Fig. 5.

modifies the chemistry and mineralogy of the protoliths (see [12]). For example, Bea and Montero [42] show that the monazite bearing granulite-facies rocks (e.g., metapelites) have higher Th/U ratios than the amphibolite-facies counterparts, indicating the preferential depletion of U due to the granulite-facies metamorphism. In addition, we find that the major rocks of the Indian Shield [6,16,43] and some granulite provinces elsewhere are also characterized by high Th/U ratios similar to the EGB.

It is well-known that the magmatic and sedimentary rocks show evidence for temporal variation of the composition of the continental crust [44–46]. In particular, these rocks show an increase of K, U and Th abundance with decreasing age. However, there is no study that includes the granulites for such tabulations. Therefore, we compile the published data of K, U and Th of the granulites of the different shield areas (Fig. 3). We find that there is no marked difference in radioelement abundances between the Archaean and Proterozoic granulites (Fig. 3). On the other hand, when Proterozoic felsic granulites (charnockites) of the EGB are compared with the late Archaean felsic granulites (gneisses and enderbites) of the Dharwar craton [6], conclusively, the EGB granulites are richer in radioelements (Fig. 3). Similarly, the felsic granulites (charnockites) of the Proterozoic Southern Granulite Terrain occurring to the south of the Dharwar craton are also richer in radioelements [16], but they are not as rich as those of the EGB granulites (Fig. 3). Therefore, the temporal variation of the radioelement abundance in the granulite-facies rocks is evident in the southern Indian Shield, but is apparently not applicable elsewhere.

3.3. Heat production

Heat production of the EGB rocks was calculated from the radioelement data using the conversion factors of Rybach [47] and is presented in Table 1. The granulites of the NEGB and SEGB have similar heat production characteristics (Fig. 4). The charnockites, gneisses and khondalites are characterized by high heat production (>2.5 μW m^{-3}), while the intermediate granulites are lower (0.55 to 1 μW m^{-3}) and the mafic granulites are the lowest (0.26 μW m^{-3}). Also, the heat production of the EGB granulites is higher, when compared to the late Archaean granulites of the adjoining Dharwar Craton (average of 0.40 μW m^{-3}) [6]. In addition, the Proterozoic granulites (charnockites and khondalites) of the Southern Granulite Terrain of the southern India are also characterized by high heat production of >1 μW m^{-3} [16]. These examples sufficiently demonstrate that the granulites are not low in heat production everywhere. Furthermore, we examine the nature of heat production of granulites occurring in the Archaean and Proterozoic shield areas elsewhere, gathering the published radioelement data (Fig. 5). We find that there are several such examples of high heat producing granulites both in the Archaean and Proterozoic provinces (Fig. 5). This observation further questions the general belief that the granulites characteristically have low heat production.

4. Present-day geotherms

4.1. Crustal contribution to the surface heat flow

For modeling the crustal temperatures, it is essential to determine the radiogenic heat contribution of the crust

Please cite this article as: P.S. Kumar et al., The role of radiogenic heat production in the thermal evolution of a Proterozoic granulite-facies orogenic belt: Eastern Ghats, Indian Shield, Earth Planet. Sci. Lett. (2006), doi:10.1016/j.epsl.2006.11.018

Table 2
The present-day crustal contribution of the Eastern Ghats to the surface heat flow

Depth layers	Rocks	Volume (%)	Heat Production ($\mu W\ m^{-3}$)	Weighted heat production ($\mu W\ m^{-3}$)	Gross heat production of layers ($\mu W\ m^{-3}$)
Northern Eastern Ghats Belt (NEGB) (35-km-thick crust)					
0–6 km (5.90 km)*	Charnockites	25	2.90	0.73	2.74
	Gneisses	50	2.78	1.39	
	Khondalites	20	2.87	0.57	
	Inter. granulites	5	1.01	0.05	
6–20 km (6.45)*	Charnockites	75	2.90	2.18	2.43
	Inter. granulites	25	1.01	0.25	
20–35 km (7.20)*	Mafic granulites	100	0.26	0.26	0.26
Southern Eastern Ghats Belt (SEGB) (40-km-thick crust)					
0–5 km (5.50–6.20)*	Charnockites	40	2.73	1.09	2.49
	Gneisses	10	2.47	0.25	
	Khondalites	40	2.76	1.10	
	Inter. granulites	7	0.55	0.04	
	Mafic granulites	3	0.26	0.01	
5–15 km (6.30–6.50)*	Charnockites	80	2.73	2.18	2.27
	Inter. granulites	15	0.55	0.08	
	Mafic granulites	5	0.26	0.01	
15–25 km (6.60)*	Inter. granulites	90	0.55	0.50	0.53
	Mafic granulites	10	0.26	0.03	
25–40 km (6.80–6.90)*	Mafic granulites	100	0.26	0.26	0.26

*Compressional wave (P-wave) velocity of layers is expressed in km s^{-1}; data source: [80,81].

by constraining the heat production variation with depth. This was done in the best way for the areas that expose crustal cross-sections. In their absence, as in the case of EGB, where the exposed rocks are only the granulite-facies rocks, it is difficult to construct the entire crustal lithology on the basis of the surface geology. However, it can possibly be deduced from the compressional wave (P-wave) velocity sections of the deep seismic sounding (DSS) studies using the laboratory P-wave velocity data of the crustal rocks (e.g. [9,79]). However, it should be remembered that this approach does not provide unique lithologic models, as several rock types can have similar P-wave velocities. Therefore, in the absence of better constraints, we model the crustal lithology of EGB using the deep seismic sounding studies [80,81] and the surface geology. To convert the P-wave velocity sections to the rock assemblages, we utilize the laboratory P-wave velocity data of the granulites [79,82]. We assign the surface heat production data to the model rock types of the deeper sections, assuming that the exposed EGB granulites extend to the Moho with varying proportions and the adjoining cratons do not merge with the EGB lithology. These assumptions are reasonable because the high-grade rocks of the EGB cannot be underlain by its low-grade rocks (which are now missing on the surface due to the erosion), and any interference of the adjoining cratonic lithology is expected only along the margins of the EGB.

Crustal lithology of the NEGB is modeled using Kaila et al. [80], who conducted the DSS studies along the Mahanadi Graben (MG). Geological mapping indicates that the basement rocks of the MG are the granulites. Therefore, it is reasonable to consider the MG crustal velocity structure to the rest of the NEGB. Crustal thickness of the MG is ~35 km and is composed of three layers with P-wave velocities of 5.9 km s^{-1}, 6.45 km s^{-1}, and 7.2 km s^{-1}, respectively, from the surface to the Moho [80] (Table 2). On the basis of the laboratory P-wave velocity data of the granulites [79,82], we interpret the DSS data in terms of lithology (Table 2) excluding the surface layer, where P-wave velocity is also controlled by other rock properties such as porosity and structural inhomogenity. Therefore, we assign the rock assemblage of the surface geology to the topmost layer, which is also in good agreement with the DSS data (Table 2). As mentioned earlier, on the basis of the assumption that the exposed granulites extend to the deeper levels with varying proportions (Table 2), we estimate the gross heat production of each layer by integrating surface heat production data and the model rock assemblages. The gross heat production is 2.74 $\mu W\ m^{-3}$, 2.43 $\mu W\ m^{-3}$ and 0.26 $\mu W\ m^{-3}$, respectively, from the surface layer (Table 2). If the above estimates

Please cite this article as: P.S. Kumar et al., The role of radiogenic heat production in the thermal evolution of a Proterozoic granulite-facies orogenic belt: Eastern Ghats, Indian Shield, Earth Planet. Sci. Lett. (2006), doi:10.1016/j.epsl.2006.11.018

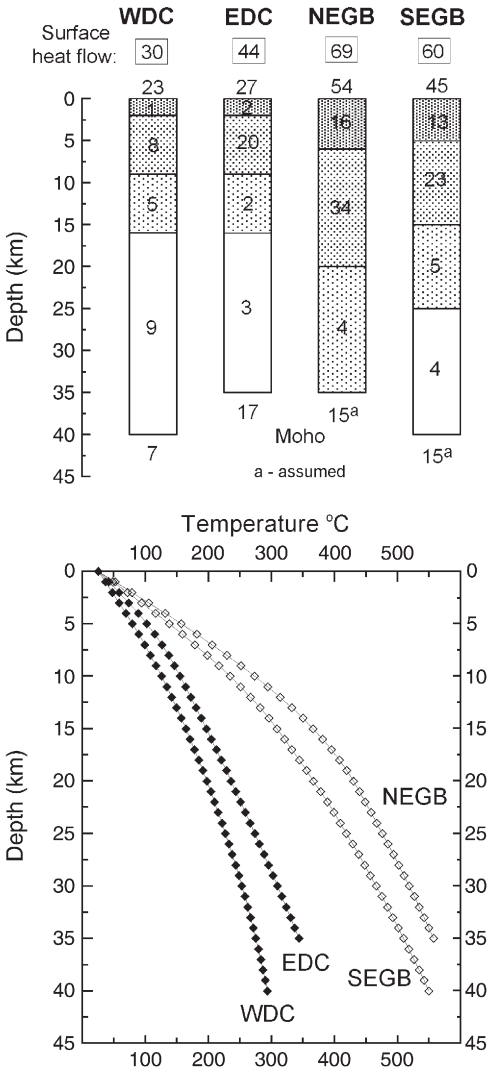

Fig. 6. Present-day crustal contribution to the surface heat flow (mW m^{-2}) and the temperature–depth profiles of the NEGB and SEGB, which are compared with the geotherms of the adjoining Dharwar craton (WDC and EDC) [6].

are realistic, then the contribution of the NEGB crust to the surface heat flow would be 54 mW m^{-2} (Fig. 6).

In the SEGB, the DSS studies were carried out in the Godavari Graben (GG) [81] and a part of which traverses the GG, where the EGB granulites form the basement. Therefore, the crustal structure belonging to the EGB basement is believed to represent the SEGB. In this part, the crustal thickness is ~40 km, and is composed of four layers with the P-wave velocities of 5.5–6.2 km s^{-1}, 6.3–6.5 km s^{-1}, 6.6 km s^{-1}, and 6.8–6.9 km s^{-1}, respectively, from the surface to the Moho (Table 2) [81]. As shown in the NEGB, we arrive at the gross heat production of each layer, which is 2.49 μW m^{-3}, 2.27 μW m^{-3}, 0.53 μW m^{-3}, and 0.26 μW m^{-3}, respectively, from the surface layer (Table 2). As a result, contribution of the SEGB to the surface heat flow is 45 mW m^{-2} (Fig. 6).

4.2. Crustal temperatures

Surface heat flow, crustal heat production and thermal conductivity constrain the crustal thermal structure. In the EGB, surface heat flow measurements are restricted to the Gondwana sedimentary basins of the Godavari graben (Fig. 2), where it ranges from 64 to 104 mW m^{-2} (n=3) [83]. If we consider the lower-bound of the surface heat flow (64 mW m^{-2}) as the representative of the SEGB and the crustal contribution of 45 mW m^{-2},then the Moho heat flow would be 19 mW m^{-2}, which seems to be reasonable considering the Moho heat flow observed in the adjoining cratons [6]. On the other hand, the upper-bound of the surface heat flow (104 mW m^{-2}) would predict the Moho heat flow of 59 mW m^{-2}, which seems to be unrealistic considering the crustal contribution model. Therefore, it appears that the crustal contribution of the NEGB is broadly in good agreement with the lower bound of the surface heat flow observed. There are no surface heat flow measurements available for the NEGB. We need to have a higher number of reliable heat flow measurements from the EGB. In absence of these, for modeling the crustal geotherms, we assume a Moho heat flow of 15 mW m^{-2} for both the NEGB and SEGB, which is the upper-bound of the Moho heat flow observed in most of the other shield areas [84]. Furthermore, using the crustal contribution models (Fig. 6) and pressure- and temperature-dependent thermal conductivity of Ketcham [5], we model the crustal geotherms of the present-day EGB adopting 1-D model assumptions, and are shown in Fig. 6. The resulting inferred Moho temperatures of the NEGB and SEGB are ~550 °C.

In Precambrian shield areas, it is generally observed that the Proterozoic provinces are characterized by higher surface heat flow compared to the Archaean cratons [85]. In the Indian shield, surface heat flow of the Eastern Ghats is higher [83], when compared to the adjoining Archaean cratons. The Dharwar craton (DC) is characterized by the surface heat flow of 30–44 mW m^{-2} [86], and in the Bastar craton it varies from 52 to 64 mW m^{-2} [87]. No surface heat flow measurements are available for the Singhbhum craton. Radiogenic heat contribution of the EGB crust varies from 45 to 54 mW m^{-2}, which is higher than in the adjoining cratons. For example, in the northern parts of the DC, contribution of

Please cite this article as: P.S. Kumar et al., The role of radiogenic heat production in the thermal evolution of a Proterozoic granulite-facies orogenic belt: Eastern Ghats, Indian Shield, Earth Planet. Sci. Lett. (2006), doi:10.1016/j.epsl.2006.11.018

Table 3
Contribution of the Eastern Ghats crust to the surface heat flow at 550 Ma ago

Depth layers	Rocks	Volume (%)	Heat production, (μW m^{-3})	Weighted heat production, (μW m^{-3})	Gross heat production of layers, (μW m^{-3})
Northern Eastern Ghats Belt (NEGB) (35-km-thick crust)					
Layer 1: 0–15 km	Model (x)	100	2.98	2.98	2.98
	Model (y)	100	1.79	1.79	1.79
Layer 2: 15–21 km	Charnockites	25	3.16	0.79	2.98
	Gneisses	50	3.03	1.52	
	Khondalites	20	3.10	0.62	
	Inter. granulites	5	1.08	0.05	
Layer 3: 21–35 km	Charnockites	75	3.16	2.37	2.64
	Inter. granulites	25	1.08	0.27	
Southern Eastern Ghats Belt (SEGB) (40-km-thick crust)					
Layer 1: 0–15 km	Model (x)	100	2.68	2.68	2.68
	Model (y)	100	1.79	1.79	1.79
Layer 2: 15–20 km	Charnockites	40	2.96	1.18	2.68
	Gneisses	10	2.67	0.27	
	Khondalites	40	2.96	1.18	
	Inter. granulites	7	0.62	0.04	
	Mafic granulites	3	0.28	0.01	
Layer 3: 20–30 km	Charnockites	80	2.96	2.37	2.47
	Inter. granulites	15	0.62	0.09	
	Mafic granulites	5	0.28	0.01	
Layer 4: 30–40 km	Inter. granulites	90	0.62	0.56	0.59
	Mafic granulites	10	0.28	0.03	

The Model (x) assumes that the heat production of the Layer 1 is same as the underlying layer 2, while the Model (y) uses the K, U and Th abundance of the upper crust of Rudnick and Gao [10].

the crust varies from 23 to 27 mW m^{-2} (Fig. 6) [6]. For comparing the EGB with the DC, we also model the crustal geotherms for the DC using the crustal contribution models shown in Fig. 6 and the temperature- and pressure-dependent thermal conductivity of Ketcham [5]. Clearly, the Moho temperatures of EGB (~550 °C) are higher than those in the DC (~300 °C) (Fig. 6).

5. Palaeo-geotherms at 550 Ma ago

In the continental crust, crustal radiogenic heat production during Precambrian was high (e.g. [20,88,89]). For example, at the end of the Archaean (~2500 Ma ago), the crustal heat production was almost double the present. Therefore, it was an important source of heat in driving the crustal metamorphism and melting in the past [17–19].In the Limpopo belt, the contrasting thermal evolution recorded in the metamorphic *P–T* data of the granulites of the northern and southern marginal zones have been attributed to their contrasting crustal radiogenic heat production [20]. Also, at many places, the contacts between the orogenic belts and the adjoining cratons are suture zones represented by the pervasive development of mylonitic rocks that preserve inverted metamorphic isograds (e.g. [90,91]). Several workers suggest that the high radiogenic heat production of the over-riding crust might have significantly contributed to the above phenomena (e.g. [92–94]).

Along the thrust contact of the EGB and the Bastar craton (Fig. 2), the footwall cratonic rocks show evidence for development of the inverted metamorphic isograds within a distance of few hundred meters toward the thrust. They preserve the metamorphic mineral assemblages pertaining to the greenschist, amphibolite and granulite-facies, respectively, from the lower to higher levels [33]. In addition, the footwall cratonic rocks exhibit progressive ductile deformation toward the thrust zone [32]. The peak metamorphic temperature in the footwall increases from 350 °C (away from the thrust zone) to 700 °C (close to the thrust zone) at a palaeo-crustal depth of ~20 km (~6.5 kbar). Whereas the hanging-wall EGB granulites record peak metamorphic temperature of >900 °C at 9.5 kbar pressure, followed by cooling and decompression to 7 kbar with 800–850 °C (retrograde metamorphism), which may be the possible thermal state of the EGB at the depth of 20–23 km, when the inverted metamorphism took place along the cratonic boundary. Based on the metamorphic *P–T* estimates, tectonic fabric, and thermal modeling,

Please cite this article as: P.S. Kumar et al., The role of radiogenic heat production in the thermal evolution of a Proterozoic granulite-facies orogenic belt: Eastern Ghats, Indian Shield, Earth Planet. Sci. Lett. (2006), doi:10.1016/j.epsl.2006.11.018

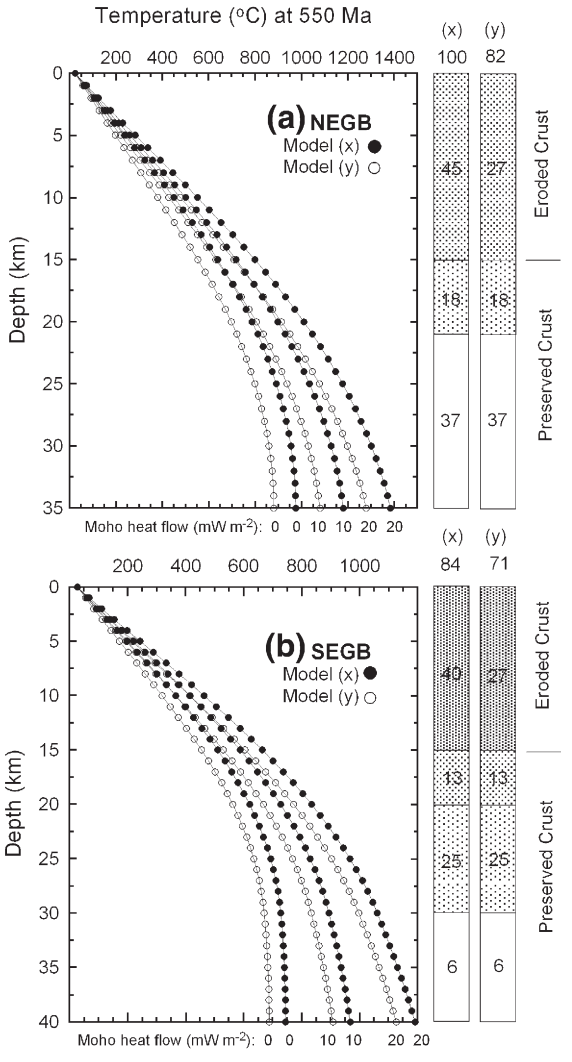

Fig. 7. Temperature–depth profiles of the NEGB and SEGB at ~550 Ma ago, for a range of Moho heat flow values (0 mW m^{-2} to 20 mW m^{-2}) and crustal heat production scenarios (model x and y). See Table 3 for crustal heat production models used in this study.

the authors [32,33] suggest that the thrusting of hot EGB crust over the cold Bastar craton could have caused the development of inverted metamorphic isograds at 550 Ma ago. We examine the crustal heat production of the EGB, in order to assess its contribution to the thermal structure of the hot EGB crust at about 550 Ma ago, considering the decay-corrected heat production data (Table 1).

5.1. Crustal contribution to the surface heat flow at 550 Ma ago

For modeling the palaeo-geotherms of the EGB, we follow the same approach as the modeling of the present-day geotherms assuming the steady-state thermal conditions (e.g. [20,88,89]). To do this, we need to know the crustal thickness, lithology and their heat production, surface heat flow or Moho heat flow at 550 Ma ago. Crustal thickness of the NEGB and SEGB is considered to be 35 km and 40 km, respectively, assuming that there was no crustal thickening. Table 3 provides the lithology of the EGB crust that includes a ~15-km-thick now-missing uppermost layer, as the present-day exposure level was at ~15 km palaeo-depth at 550 Ma ago. The uppermost layer is underlain by the crustal layers of the present-day crust without the lowermost mafic layer (Table 2) (Fig. 6). We do not include this mafic layer in the palaeo-crustal configuration because this would lead to significant crustal thickening. Inclusion or omission of the mafic layer would not significantly modify the thermal models in the depth-levels of our interest (~20-km-depth) as they would have very low heat production (e.g., <0.3 μW m^{-3}). We assign the decay-corrected heat production data to these layers (Table 1). For the heat production of the now-missing uppermost layer, we consider two scenarios: (1) Model x: the layer may have heat production similar to the present-day exposed rocks (i.e., the second granulite-facies layer of the 550 Ma ago crust); (2) Model y: the layer may have heat production

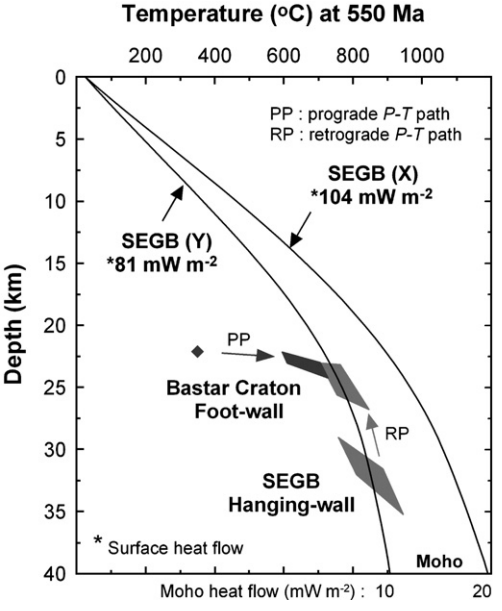

Fig. 8. A comparison between the metamorphic *P–T* data (the SEGB hanging-wall granulites and the cratonic footwall gneisses [33]) and the 550 Ma ago geotherms of the SEGB (Fig. 7b). Note that the geotherm pertaining to the crustal contribution model (Y) with the Moho heat flow value of 10 mW m^{-2} better represents the metamorphic conditions of the EGB hanging-wall granulites.

Please cite this article as: P.S. Kumar et al., The role of radiogenic heat production in the thermal evolution of a Proterozoic granulite-facies orogenic belt: Eastern Ghats, Indian Shield, Earth Planet. Sci. Lett. (2006), doi:10.1016/j.epsl.2006.11.018

similar to the generic composition model of the Proterozoic upper crust, as suggested by Rudnick and Gao [10]. Both these models are reasonable. For example, a few exposed crustal cross-sections indicate that the amphibolite-facies rocks (similar to the uppermost layer) resting on the granulite-facies rocks (similar to the second layer) have heat production same as the granulites [95]. Also, Rudnick and Gao [10] modeled the composition of Proterozoic upper crust considering the global geochemical database. Hence, we consider both the possibilities. Assigning the decay-corrected heat production data to the crustal layers, we show the crustal contribution of the NEGB and SEGB to be 100 mW m^{-2} and 84 mW m^{-2}, respectively, for the model x (Fig. 7). On the other hand, if we assume the model y, it would be 82 mW m^{-2} and 71 mW m^{-2}, respectively (Fig. 7). Uncertainties in these estimates cannot be determined.

5.2. Crustal temperatures at 550 Ma ago

Using the crustal contribution models (Table 3), variable Moho heat flow (0, 10, and 20 mW m^{-2}) and *P–T* dependent thermal conductivity [5], we model the crustal geotherms of the NEGB and SEGB (Fig. 7). The Moho temperatures of the NEGB vary from 800 °C to 1400 °C, and in the SEGB from 700 °C to 1200 °C (Fig. 7). These model temperatures are distinctly higher than those at the corresponding depth levels of the present-day geotherms (Fig. 6). We further examine these geotherms (Fig. 7), in order to find out the one that would represent the metamorphic *P–T* data of the EGB granulites (Fig. 8). As the inverted metamorphic isograds are observed in the northwestern boundary of the SEGB (Fig. 2), it is pertinent to compare the metamorphic *P–T* data with the geotherms of the SEGB (Fig. 7b). Of the many geotherms, the one that passes through the metamorphic *P–T* data is the geotherm, which includes the crustal model y and the Moho heat flow of 10 mW m^{-2} (Fig. 8). Therefore, it supports a possibility that the high crustal heat production with normal Moho heat flow could have been responsible for the hot thermal condition of the EGB at 550 Ma ago, which might have caused the development of inverted metamorphism along its contact with the adjoining cratons, during the collisional orogenic event at about 550 Ma ago.

Acknowledgements

The authors sincerely thank Richard A. Ketcham for the helpful comments; Claude Jaupart for editorial handling and suggestions; J.-C. Mareschal for the useful suggestions on an earlier version of the manuscript; Pulak Sengupta for stimulating discussions; T. Seshunarayana, C. Shankar and G. Ramacharyulu for the support; V. P. Dimri, Director, NGRI for the permission to publish this paper.

References

[1] C. Jaupart, J.-C. Mareschal, Constraints on crustal heat production from heat flow data, in: R.L. Rudnick (Ed.), The Crust, vol. 3, Treatise on Geochemistry (eds.H.D. Holland and K.K. Turekian), Elsevier-Pergamon, Oxford, 2003, pp. 65–84.

[2] D.M. Fountain, M.H. Salisbury, K.P. Furlong, Heat production and thermal conductivity of rocks from the Pikwitonei–Sachigo continental cross section, central Manitoba: implications for the thermal structure of Archaean crust, Can. J. Earth Sci. 24 (1987) 1583–1594.

[3] C. Pinet, C. Jaupart, The vertical distribution of radiogenic heat production in the Precambrian crust of Norway and Sweden: geothermal implications, Geophys. Res. Lett. 14 (1987) 260–263.

[4] L.D. Ashwal, P. Morgan, S.A. Kelley, J.A. Percival, Heat production in an Archaean crustal profile and implications for heat flow and mobilization of heat-producing elements, Earth Planet. Sci. Lett. 85 (1987) 439–450.

[5] R.A. Ketcham, Distribution of heat-producing elements in the upper and middle crust of southern and west central Arizona: evidence from core complexes, J. Geophys. Res. 101 (1996) 13611–13632.

[6] P.S. Kumar, G.K. Reddy, Radioelements and heat production of an exposed cross-section of Archaean crust, Dharwar craton, south India, Earth Planet. Sci. Lett. 224 (2004) 309–324.

[7] R.J. Brady, M.N. Ducea, S.B. Kidder, J.B. Saleeby, The distribution of radiogenic heat production as a function of depth in the Sierra Nevada Batholith, California, Lithos 86 (2006) 229–244.

[8] S.L. Harley, The origins of granulites: a metamorphic perspective, Geol. Mag. 126 (1989) 215–247.

[9] R.L. Rudnick, D.M. Fountain, Nature and composition of the continental crust: a lower crustal perspective, Rev. Geophys. 33 (1995) 267–309.

[10] R.L. Rudnick, S. Gao, Composition of continental crust, in: R.L. Rudnick (Ed.), The Crust, vol. 3, Treatise on Geochemistry (eds. H.D. Holland and K.K. Turekian), Elsevier-Pergamon, Oxford, 2003, pp. 1–64.

[11] D.M. Fountain, R. Arculus, R.W. Kay (Eds), Cotinental Lower Crust, Developments in Geotectonics 23, Elsevier, Amsterdam, 1992, 485 pp.

[12] H.R. Rollinson, J. Tarney, Adakites — the key to understanding LILE depletion in granulites, Lithos 79 (2005) 61–81.

[13] W.S. Fyfe, The granulite facies, partial melting and the Archaean crust, Philos. Trans. R. Soc. Lond. A273 (1973) 457–462.

[14] R.C. Newton, L.Ya. Aranovich, E.C. Hansen, B.A. Vandenheuvel, Hypersaline fluids in Precambrian deep-crustal metamorphism, Precambrian Res. 91 (1998) 41–63.

[15] M.J. Drury, Heat flow in the Canadian shield and its relation to other geophysical parameters, in: V. Cermak, L. Rybach (Eds.), Terrestrial Heat Flow and the Lithospheric Structure, Springer-Verlag, New York, 1991, pp. 317–337.

[16] L. Ray, P.S. Kumar, G.K. Reddy, S. Roy, G.V. Rao, R. Srinivasan, R.U.M. Rao, High mantle heat flow in a Precambrian

Please cite this article as: P.S. Kumar et al., The role of radiogenic heat production in the thermal evolution of a Proterozoic granulite-facies orogenic belt: Eastern Ghats, Indian Shield, Earth Planet. Sci. Lett. (2006), doi:10.1016/j.epsl.2006.11.018

granulite province: evidence from southern India, J. Geophys. Res. 108 (B2) (2003) 2084, doi:10.1029/2001JB000688.

[17] C.P. Chamberlain, L.S. Sonder, Heat-producing elements and thermal and baric patterns of metamorphic belts, Science 250 (1990) 763–769.

[18] M. Sandiford, M. Hand, S. McLaren, High geothermal gradient metamorphism during thermal subsidence, Earth Planet. Sci. Lett. 163 (1998) 149–165.

[19] S. McLaren, M. Sandiford, M. Hand, High radiogenic heat-producing granites and metamorphism — an example from the western Mount Isa inlier, Australia, Geology 27 (1999) 679–682.

[20] J.D. Kramers, K. Kreissig, M.Q.W. Jones, Crustal heat production and style of metamorphism: a comparison between two Archaean high grade provinces in the Limpopo Belt, southern Africa, Precambrian Res. 112 (2001) 149–163.

[21] C.J. Dobmeier, M.M. Raith, Crustal architecture, and evolution of the Eastern Ghats belt and adjacent regions of India, in: M. Yoshida, B.F. Windley, S. Dasgupta (Eds.), Proterozoic East Gondwana: Supercontinent Assembly and Breakup, vol. 206, Geological Society of London, London, 2003, pp. 145–168.

[22] K. Rickers, K. Mezger, M.M. Raith, Evolution of the continental crust in the Proterozoic Eastern Ghats belt, India and new constraints for Rodina reconstruction: implications from Sm–Nd, Rb–Sr, and Pb–Pb isotopes, Precambrian Res. 112 (2001) 183–210.

[23] T.R.K. Chetty, D.S.N. Murthy, Collisional tectonics in the late Precambrian Eastern Ghats Mobile Belt: mesoscopic to satellite-scale structural observations, Terra Nova 6 (1994) 72–81.

[24] S. Bhattacharya, Evolution of Eastern Ghats granulite belt of India in compressional tectonic regime and juxtaposition against iron ore craton of Singhbhum by oblique collision–transpression, Proc. Indian Acad. Sci., A Earth Planet. Sci. 106 (1997) 65–75.

[25] D.K. Paul, T.R. Barman, N.J. McNaughton, I.R. Fletcher, P.J. Potts, M. Ramakrishnan, P.F. Augustine, Archaean–Proterozoic evolution of Indian charnockites: isotopic and geochemical evidence from granulites of the Eastern Ghats belts, J. Geol. 98 (1990) 253–263.

[26] K. Mezger, M.A. Cosca, The thermal history of the Eastern Ghat belt (India) as revealed by U–Pb and $^{40}Ar/^{39}Ar$ dating of metamorphic and magmatic minerals: implications for the SWEAT correlation, Precambrian Res. 94 (1999) 251–271.

[27] W.A. Crowe, M.A. Cosca, L.B. Harris, $^{40}Ar/^{39}Ar$ geochronology and Neoproterozoic tectonics along the northern margin of the Eastern Ghats belt in north Orissa, Precambrian Res. 108 (2001) 237–266.

[28] F. Lisker, S. Fachmann, Phanerozoic history of the Mahanadi region, India, J. Geophys. Res. 106 (2001) 22027–22050.

[29] S. Dasgupta, P. Sengupta, Indo-Antarctic correlation: a perspective from the Eastern Ghats Granulite belt, India, in: M. Yoshida, B.F. Windley, S. Dasgupta (Eds.), Proterozoic East Gondwana: Supercontinent Assembly and Breakup, vol. 206, Geological Society of London, London, 2003, pp. 131–143.

[30] G.N. Rao, Sedimentation, stratigraphy, and petroleum potential of Krishna–Godavari basin, east coast of India, Am. Assoc. Pet. Geol. Bull. 85 (2001) 1623–1643.

[31] T. Okudaira, T. Hamamoto, B.H. Prasad, R. Kumar, Sm–Nd and Rb–Sr dating of amphibolite from the Nellore–Khammam schist belt, SE India: constraints on the collision of the Eastern Ghats terrane and Dharwar–Bastar craton, Geol. Mag. 138 (2001) 495–498.

[32] S. Bhadra, S. Gupta, M. Banerjee, Structural evolution across the Eastern Ghats Mobile Belt–Bastar Craton boundary, India: hot over cold thrusting in an ancient collision zone, J. Structural Geol. 26 (2004) 233–245.

[33] S. Gupta, A. Bhattacharya, M. Raith, J.K. Nanda, Contrasting pressure–temperature-deformation history across a vestigal craton-mobile belt boundary: the western margin of the Eastern Ghats belt at Deobhog, India, J. Metamorph. Geol. 18 (2000) 683–697.

[34] P. Sengupta, J. Sen, S. Dasgupta, M. Raith, U.K. Bhui, J. Ehl, Ultra-high temperature metamorphism of metapelitic granulites from Kondapalle, Eastern Ghats belt: implications for the Indo-Antartic correlation, J. Petrol. 40 (1999) 1065–1087.

[35] F. Lisker, R. Brown, D. Fabel, Denudational and thermal history along a transect across the Lambert Graben, northern Prince Charles Mountains, Antarctica, derived from apatite fission track thermochronology, Tectonics 22 (5) (2003) 1055, doi:10.1029/2002TC001477.

[36] M. Yoshida, B.F. Windley, S. Dasgupta (Eds.), Proterozoic East Gondwana: Supercontinental Assembly and Breakup, Geological Society, London, Special Publications, vol. 206, 2003, 472 pp.

[37] K.S. Prakasam, S.S. Rai, Teleseismic delay-time tomography of the upper mantle beneath southeastern India: imprint of Indo-Antartic rifting, Geophys. J. Int. 133 (1998) 20–30.

[38] Geological Map of India, Scale 1:2000000, Geological Survey of India, Kolkata, 1998.

[39] R.A. Ketcham, An improved method for determination of heat production with gamma-ray scintillation spectrometry, Chem. Geol. 130 (1996) 175–194.

[40] R.G. Rao, P. Sahoo, N.K. Panda, Heavy mineral deposits of Orissa, in: R.D. Raju, M.A. Ali, S. Krishnan (Eds.), Beach and Inland Heavy Mineral Sand Deposits of Andhra Pradesh, Expl. Res. Atomic Minerals, vol. 13, 2001, pp. 23–52.

[41] G.S. Ravi, R.G. Rao, A.Y. Rao, Coastal heavy mineral sand deposits of Andhra Pradesh, in: R.D. Raju, M.A. Ali, S. Krishnan (Eds.), Beach and Inland Heavy Mineral Sand Deposits of Andhra Pradesh, Expl. Res. Atomic Minerals, vol. 13, 2001, pp. 53–85.

[42] F. Bea, P. Montero, Behavior of accessory phases and redistribution of Zr, REE, Y, Th, and U during metamorphism and partial melting of metapelites in the lower crust: an example from the Kinzigite formation of Ivrea-Verbano, NW Italy, Geochim. Cosmochim. Acta 63 (1999) 1133–1153.

[43] R. Menon, P.S. Kumar, G.K. Reddy, R. Srinivasan, Radiogenic heat production of late Archaean Bundelkhand granite and some Proterozoic gneisses and granitoids of central India, Curr. Sci. 85 (2003) 634–638.

[44] S.R. Taylor, S.M. McLennan, The Continental Crust: its Composition and Evolution, Blackwell, Oxford, 1985, 312 pp.

[45] M. Meyer, L.J. Robb, C.R. Anhaeusser, Uranium and thorium contents of Archaean granitoids from the Barberton Mountain Land, South Africa, Precambrian Res. 33 (1986) 303–321.

[46] H. Martin, J.-F. Moyen, Secular changes in tonalite–trondhjemite–granodiorite composition as markers of the progressive cooling of earth, Geology 30 (2002) 319–322.

[47] L. Rybach, Determination of heat production rate, in: R. Haenel, L. Rybach, L. Stegena (Eds.), Handbook of Terrestrial Heat Flow Determination, Kluwer, Dordrecht, 1988, pp. 125–142.

[48] P. Holtta, Geochemical characteristics of granulite facies rocks in the Archean Varpaisjarvi area, central Fennoscandian Shield, Lithos 40 (1997) 31–53.

[49] J.-C. Mareschal, A. Poirier, F. Rolandone, G. Bienfait, C. Gariepy, R. Lapointe, C. Jaupart, Low mantle heat flow at the edge of the North American continent, Voisey Bay, Labrador, Geophys. Res. Lett. 27 (2000) 823–826.

[50] A. Joeleht, I.T. Kukkonen, Thermal properties of granulite facies rocks in the Precambrian basement of Finland and Estonia, Tectonophysics 291 (1998) 195–203.

Please cite this article as: P.S. Kumar et al., The role of radiogenic heat production in the thermal evolution of a Proterozoic granulite-facies orogenic belt: Eastern Ghats, Indian Shield, Earth Planet. Sci. Lett. (2006), doi:10.1016/j.epsl.2006.11.018

[51] S. Gao, T.-C. Luo, B.-R. Zhang, H.-F. Zhang, Y.-W. Han, Z.-D. Zhao, Y.-K. Hu, Chemical composition of the continental crust as revealed by studies in East China, Geochim. Cosmochim. Acta 62 (1998) 1959–1975.

[52] J.A. Percival, J.K. Mortensen, Water-deficient calc-alkaline plutonic rocks of northeastern Superior province, Canada: significance of charnockitic magmatism, J. Petrol. 43 (2002) 1617–1650.

[53] J.W. Sheraton, L.P. Black, Geochemistry of Precambrian gneisses: relevance for the evolution of the East Antarctic Shield, Lithos 16 (1983) 273–296.

[54] M. Berger, H. Rollinson, Isotopic and geochemical evidence for crust–mantle interaction during late Archaean crustal growth, Geochim. Cosmochim. Acta 61 (1997) 4809–4829.

[55] S.P. Johnson, H.N.C. Cutten, S. Muhongo, B.D. Waele, Neoarchaean magmatism and metamorphism of the western granulites in the central domain of the Mozambique belt, Tanzania: U–Pb shrimp geochronology and P–T estimates, Tectonophysics 375 (2003) 125–145.

[56] S.S. Iyer, A. Choudhuri, M.B.A. Vasconcellos, U.G. Cordani, Radioactive element distribution in the Archean granulite terrane of Jequie-Bahia, Brazil, Contrib. Mineral. Petrol. 85 (1984) 95–101.

[57] G.P. Sighinolfi, M.C.H. Figueredo, W.S. Fyfe, B.I. Kronberg, M.A.F.T. Oliveira, Geochemistry and petrology of the Jequie granulitic complex (Brazil): an Archaean basement complex, Contrib. Mineral. Petrol. 78 (1981) 263–271.

[58] K. Kreissig, T.F. Nägler, J.D. Kramers, D.D. van Reenen, C.A. Smit, An isotopic and geochemical study of the northern Kaapvaal Craton and the Southern Marginal Zone of the Limpopo Belt: are they juxtaposed terranes? Lithos 50 (2000) 1–25.

[59] S.R. Taylor, R.L. Rudnick, S.M. McLennan, K.A. Eriksson, Rare earth element patterns in Archaean high-grade meta-sediments and their tectonic significance, Geochim. Cosmochim. Acta 50 (1986) 2267–2279.

[60] P.J. Lawlor, F.O. Gutierrez, K.L. Cameron, H. Ochoa-Camarillo, R. Lopez, D.E. Sampson, U–Pb geochronology, geochemistry, and provenance of the Grenvillian Huiznopala Gneiss of Eastern Mexico, Precambrian Res. 94 (1999) 73–99.

[61] O. Blein, M.R. LaFleche, L. Corriveau, Geochemistry of the granulitic Bondy gneiss complex: a 1.4 Ga arc in the central metasedimentary belt, Grenville Province, Canada, Precambrian Res. 120 (2003) 193–217.

[62] K.S. Heier, J.A.S. Adams, Concentration of radioactive elements in deep crustal material, Geochim. Cosmochim. Acta 29 (1965) 53–61.

[63] B. Weber, L. Hecht, Petrology and geochemistry of metaigneous rocks from a Grenvillian basement fragment in the Maya block: the Guichicovi complex, Oaxaca, southern Mexico, Precambrian Res. 124 (2003) 41–67.

[64] S.B. Smithson, K.S. Heier, U, and Th distribution between normal and charnockitic facies of a deep granitic intrusion, Earth Planet. Sci. Lett. 12 (1971) 325–326.

[65] K.S. Heier, K. Thorensen, Geochemistry of high grade metamorphic rocks, Lofoten–Vesteralen, North Norway, Geochim. Cosmochim. Acta 35 (1971) 89–99.

[66] S.S. Hughes, S.E. Lewis, M.J. Bartholomew, A.K. Sinha, T.A. Hudson, N. Herz, Chemical diversity and origin of Precambrian charnockitic rocks of the central Pedlar massif, Grenvillian blue ridge terrane, Virginia, Precambrian Res. 84 (1997) 37–62.

[67] S.S. Iyer, A. Choudhuri, D.R.M. Pattison, G.R. De Paoli, Petrology and geochemistry of the Neoproterozoic Guaxupe granulite facies terrain, southeastern Brazil, Precambrian Res. 77 (1996) 23–40.

[68] D. Demaiffe, J.-C. Duchesne, J. Hertogen, Trace element variations and isotopic composition of charnockitic acidic rocks related to anorthosites (Rogaland, S.W. Norway), in: L.H. Ahrens (Ed.), The Origin and Distribution of the Elements, Pergamon, 1979, pp. 417–429.

[69] D.N. Young, J. Zhao, D.J. Ellis, M.T. McCulloch, Geochemical and Sr–Nd isotopic mapping of source provinces for the Mawson charnockites, east Antarctica: implications for Proterozoic tectonics and Gondwana reconstruction, Precambrian Res. 86 (1997) 1–19.

[70] X.Q. Zhou, B. Bingen, D. Demaiffe, J.P. Liegeois, J. Hertogen, D. Weis, J. Michot, The 1160 Ma Hidderskog meta-charnockite: implications of this A-type pluton for the Sveconorwegian belt in Vest Agder (SW Norway), Lithos 36 (1995) 51–66.

[71] I.T. Kukkonen, A. Joehlet, Geothermal modeling of the lithosphere in the central Baltic Shield and its southern slope, Tectononphysics 255 (1996) 25–45.

[72] C.M. Gray, The geochemistry of central Australian granulites in relation to the chemical and isotopic effects of granulite facies metamorphism, Contrib. Mineral. Petrol. 65 (1977) 79–89.

[73] J. Zhao, D.J. Ellis, J.A. Kilpatrick, M.T. McCulloch, Geochemical and Sr–Nd isotopic study of charnockites and related rocks in the northern Prince Charles mountains, East Antarctica: implications for charnockite petrogenesis and Proterozoic crustal evolution, Precambrian Res. 81 (1997) 37–66.

[74] J.B. Griffiths, S. Fourcade, J.-R. Kienast, J.-J. Peucat, F. Martineau, A. Rahmani, Geochemistry and isotope (Sr, Nd, O) study of Al–Mg granulites from the In Ouzzal Archaean block, Algeria, J. Metamorph. Geol. 14 (1996) 709–724.

[75] T.L. Knudsen, T. Andersen, C. Maijer, R.H. Verschure, Trace-element characteristics and Pb isotopic evolution of metasediments and associated Proterozoic rocks from the amphibolite- to granulite facies Bamble sector, southern Norway, Chem. Geol. 143 (1997) 145–169.

[76] B. Schnetger, Partial melting during the evolution of the amphibolite- to granulite-facies gneisses of the Iverea Zone, northern Italy, Chem. Geol. 113 (1994) 71–101.

[77] D.P. Windrim, M.T. McCulloch, B.W. Chappell, W.E. Cameron, Nd isotopic systematics and chemistry of Central Australian sapphirine granulites: an example of rare earth element mobility, Earth Planet. Sci. Lett. 70 (1984) 27–39.

[78] M.A.G. Andreoli, R.J. Hart, L.D. Ashwal, H. Coetzee, Correlations between U, Th content and metamorphic grade in the western Namaqualand belt, South Africa, with implications for radioactive heating of the crust, J. Petrol. 47 (2006) 1095–1118.

[79] N.I. Christensen, W.D. Mooney, Seismic velocity structure and composition of the continental crust: a global review, J. Geophys. Res. 100 (1995) 9761–9788.

[80] K.L. Kaila, H.C. Tiwari, D.M. Mall, Crustal structure and delineation of Gondwana basin in the Mahanadi delta area, India from deep seismic sounding, J. Geol. Soc. India 29 (1987) 293–308.

[81] K.L. Kaila, P.R.K. Murty, V.K. Rao, N. Venkateswarlu, Deep seismic sounding in the Godavari graben and Godavari (coastal) basin, India, Tectonophysics 173 (1990) 307–317.

[82] N.I. Christensen, Poisson's ratio and crustal seismology, J. Geophys. Res. 101 (1996) 3139–3156.

[83] G.V. Rao, R.U.M. Rao, Heat flow in the Indian Gondwana basins and heat production of their basement rocks, Tectonophysics 91 (1983) 105–117.

Please cite this article as: P.S. Kumar et al., The role of radiogenic heat production in the thermal evolution of a Proterozoic granulite-facies orogenic belt: Eastern Ghats, Indian Shield, Earth Planet. Sci. Lett. (2006), doi:10.1016/j.epsl.2006.11.018

[84] C. Jaupart, J.-C. Mareschal, L.G. Frottier, A. Davaille, Heat flow and thickness of the lithosphere in the Canadian shield, J. Geophys. Res. 103 (1998) 15269–15286.
[85] A.A. Nyblade, H.N. Pollack, A global analysis of heat flow from Precambrian terrains: implications for the thermal structure of Archaean and Proterozoic lithosphere, J. Geophys. Res. 98 (1993) 12207–12218.
[86] S. Roy, R.U.M. Rao, Towards a crustal thermal model for the Archaean Dharwar craton, southern India, Phys. Chem. Earth 28 (2003) 361–373.
[87] M.L. Gupta, A. Sundar, S.R. Sharma, S.B. Singh, Heat flow in the Bastar craton, central Indian shield: implications for thermal characteristics of Proterozoic cratons, Phys. Earth Planet. Inter. 78 (1993) 23–31.
[88] J.-C. Mareschal, C. Jaupart, Archaean thermal regime and stabilization of the cratons, in: K. Benn, K.C. Condie, J.-C. Mareschal (Eds.), Archaean Geodynamic Processes, AGU, Washington D.C., 2006, pp. 61–73.
[89] H.K.C. Perry, J.-C. Mareschal, C. Jaupart, Variations of strength and localized deformation in cratons: the 1.9 Ga Kapuskasing uplift, Superior Province, Canada, Earth Planet. Sci. Lett. 249 (2006) 216–228.
[90] P.G. Anderson, B. Lagerblad, Occurrence and significance of inverted metamorphic gradients in the western Scandinavian Caledonides, J. Geol. Soc. (Lond.) 137 (1980) 219–230.
[91] E.M. Duebendorfer, Evidence for an inverted metamorphic gradient associated with a Precambrian suture, southwestern Wyoming, J. Metamorph. Geol. 6 (1988) 41–63.
[92] C. Jaupart, A. Provost, Heat focussing, granite genesis and inverted metamorphic gradients in continental collision zones, Earth Planet. Sci. Lett. 73 (1985) 385–397.
[93] C. Pinet, C. Jaupart, A thermal model for the distribution in space and time of the Himalayan granites, Earth Planet. Sci. Lett. 84 (1987) 87–99.
[94] A.D. Huerta, L.H. Royden, K.V. Hodges, The thermal structure of collisional orogens as a response to accretion, erosion and radiogenic heating, J. Geophys. Res. 103 (1998) 15287–15302.
[95] B. Bingen, D. Demaiffe, J. Hertogen, Redistribution of rare earth elements, thorium, and uranium over accessory minerals in the course of amphibolite to granulite facies metamorphism: the role of apatite and monazite in orthogneisses from southwestern Norway, Geochim. Cosmochim. Acta 60 (1996) 1341–1354.

Please cite this article as: P.S. Kumar et al., The role of radiogenic heat production in the thermal evolution of a Proterozoic granulite-facies orogenic belt: Eastern Ghats, Indian Shield, Earth Planet. Sci. Lett. (2006), doi:10.1016/j.epsl.2006.11.018